DOI 10.1007/s11182-023-02989-y
Russian Physics Journal, Vol. 66, No. 6, October, 2023

OPTICS AND SPECTROSCOPY

INFLUENCE OF Tm^{3+} CONCENTRATION ON LONG AFTERGLOW AND PHOTOSTIMULATED LUMINESCENCE PROPERTIES OF Eu^{2+}-DOPED $Sr_1Al_2Si_2O_8$ BLUE PHOSPHORS

S. Y. Liu,[1] D. Gao,[2] L. Wang,[1] W. B. Song,[1] Q. M. Yu,[1] Y. B. Wen,[1] and X. L. Zhang[1] UDC 535.8

Blue aluminum silicate phosphors of $Sr_1Al_2Si_2O_8$, $Sr_{0.98}Al_2Si_2O_8$:$0.02Eu^{2+}$ *and* $Sr_{0.98-x}Al_2Si_2O_8$:$0.02Eu^{2+}$, xTm^{3+} *(x = 0.005, 0.01, 0.02, 0.04, 0.08) compositions are prepared by high temperature solid phase method. Their XRD, fluorescence emission and excitation luminescence properties, afterglow attenuation, afterglow luminescence, thermoluminescence and photostimulated luminescence properties are investigated. The results show that a high purity crystallized phosphor can be successfully prepared at 1350°C for 4 h. It is proven that* Eu^{2+} *as the luminescent center is replaced by* Sr^{2+} *with a coordination number of 12;* Eu^{2+} *and* Tm^{3+} *are substituted for* Sr^{2+}*, which is the reason for a decrease in the unit cell parameter values. The sample excitation and emission spectra have peak wavelengths of 330 nm and 405 nm.* $Sr_{0.97}Al_2Si_2O_8$:$0.02Eu^{2+}$, $0.01Tm^{3+}$ *has a minimum afterglow decay rate of 0.61389, which is suitable for use as a long-lasting luminescent blue phosphor. The pyroluminescence indicates that doping with* Tm^{3+} *significantly deepens the trap level. The photostimulated luminescence proves that the co-doped* Tm^{3+} *greatly improves the initial intensity and the optical storage performance of the photostimulated luminescence, especially the* $Sr_{0.96}Al_2Si_2O_8$:$0.02Eu^{2+}$*; the* $0.02Tm^{3+}$ *sample trap level is 0.8999 eV. The initial photostimulated luminescence intensity of the co-doped sample is shown to be 1000 times that of the single doped* Eu^{2+}*, and the optical storage – 1.8 times that of the single doping case.*

Keywords: optical storage, photostimulated luminescence, deep trap level, blue LED, $Sr_{0.96}Al_2Si_2O_8$.

INTRODUCTION

Photostimulated materials are also known as the electron trapping materials (ETMs), which were first proposed and applied by Lindmayer far back in 1988 [1–5]. A photostimulated material belongs to wide bandgap compound materials doped with one or more rare earth elements in a suitable matrix material. This material gets high energy for a long time when it is excited. It can generate electron or hole traps, which in turn gives rise to an objective long-term energy storage; that is why it is named an ETM. With the rapid development of the electronics industry, photostimulated materials have been used in infrared detection [6, 7], radiation dose measurement [8], optical storage [9–11], optical information readout and information field applications [12, 13]. This has greatly enabled researchers to see the broad prospects for the development of optoelectronic information materials. Note that the use of photostimulated materials in the field of infrared detection can provide a low response threshold and a high response range. Moreover, optical excitation materials are also important in the field of optical information storage, offering numerous advantages. This is especially relevant for the photoelectric information storage, due to the characteristics of

[1]School of Intelligence and Electronic Engineering, Dalian Neusoft University of Information, Dalian, China, e-mail: liushengyi@mail.ru; liushengyi@neusoft.edu.cn; [2]College of Science, Dalian Maritime University, Dalian, China. Original article submitted September 3, 2023.

fast reading, high storage density, easy erasing and multiple multiplexing [14, 15]. The phenomenon of photostimulated luminescence can be simply understood as a transition of electrons from the valence band to the conduction band to generate holes and free electrons when the material is excited. In a certain period of time, the holes and free electrons trapped by the electrons are quickly excited from the trap to the local level of the luminescent center ions, when excited by infrared light, and are released at a certain wavelength [16]. The long afterglow luminescence is a phenomenon where the material can continue emitting light when the ionizing radiation is removed after a certain period of exposure. The reason for this is the process of releasing and recombining the trapped carriers under a thermal disturbance by the excitation-generated traps in the material at room temperature [17–19]. The researchers have recently made tremendous efforts on finding photostimulated luminescent materials in view of a wide range of their applications. Among them, metal halides and sulfides as matrix materials are doped with rare earth elements to prepare more photostimulated storage materials [20], such as: $KCaSO_4Cl:Ln^{3+}$ (Ln = Dy, Ce, Pb, Mn). The thermoluminescence properties were first discovered by Gedam et al. [21] and also reported by Y. Kojima et al. ($SrS:Eu^{2+}$, Pr^{3+} materials) [22], Manashirov et al. and Shuang et al. ($SrS:Eu^{2+}$ and Sm^{3+} sulfide systems) [23, 24]. However, the earliest studied alkaline earth metal sulfide and halide systems have been by now replaced by alkaline earth metal silicate systems developed in recent years due to their chemical properties, poor thermal stability and environmental friendliness. Among them, $Sr_3SiO_5:Eu^{2+}$, Tm^{3+} yellow light excitation materials have been reported by Liu et al. [3]. In recent years, it has been found out that co-doped rare earth elements can transform the defects of silicates into the traps for energy storage [25]. Zhang and Sun et al. [26, 27] reported that $Sr_3SiO_5:Eu^{2+}$, Dy^{3+} phosphors have deeper trap levels and demonstrate better photostimulated properties. The photostimulated luminescent materials with aluminosilicate matrices are poorly studied either, and the long afterglow and photostimulated properties of Tm^{3+}-doped $Sr_1Al_2Si_2O_8$ have not been reported, to our knowledge.

In this paper, we discuss the $Sr_{0.98}Al_2Si_2O_8:0.02Eu^{2+}$ phosphors doped with different Tm^{3+} concentrations prepared by a high-temperature solid-phase method and study the effects of different Tm^{3+} content on its long-lasting luminescence properties. The pyroluminescence spectra were measured by an F-4600 fluorescence spectrometer. The trap energy levels of thermoluminescence were calculated by the Chen model. The sample was excited using a 980 nm infrared laser, and the photostimulated initial luminescence intensity was measured and recorded. The energy storage characteristics of $Sr_{0.98}Al_2Si_2O_8:0.02Eu^{2+}$ doped with different Tm^{3+} concentrations were compared, and the luminescence mechanism of the photostimulated material was interpreted based on the energy storage characteristics. The photostimulated alternating curves were tested to further verify the energy storage characteristics of different Tm^{3+}-doped $Sr_{0.98}Al_2Si_2O_8:0.02Eu^{2+}$ samples.

EXPERIMENTAL

Experimental materials and equipment

The chemical reagent Al_2O_3 for the research group was purchased from Tianjin Guangfun Fine Chemical Research Institute; $SrCO_3$ was purchased from Sinopharm Chemical Reagent Co., Ltd.; SiO_2 was purchased from Tianjin Jinbei Fine Chemical Co., Ltd.; and Eu_2O_3(99.99%) and Tm_2O_3(99.99%) were purchased from Tianjin Jinke Fine Chemical Research Institute. An aluminum oxide crucible was used in the test vessel. The equipment in this experiment was a Tianjin central electric production muffle furnace operating at a temperature of 1600°C.

Experimental procedure and parameters

Seven samples of $Sr_1Al_2Si_2O_8$, $Sr_{0.98}Al_2Si_2O_8:0.02Eu^{2+}$ and $Sr_{0.98-x}Al_2Si_2O_8:0.02Eu^{2+}$, xTm^{3+} (x = 0.005, 0.01, 0.02, 0.04, 0.08) were prepared by a high-temperature solid-phase synthesis. First, the chemical reagents $SrCO_3$, Al_2O_3, SiO_2, Eu_2O_3 and Tm_2O_3 were weighed according to a certain stoichiometric ratio. Each part was placed in an agate mortar for 30 minutes, ground and placed in an Al_2O_3 crucible to be incubated at 1350°C for 4 hrs in a CO atmosphere in a muffle furnace. After the sample was cooled to a room temperature of 30°C, it was poured into an agate mortar and carefully ground and placed in a sample bag for testing.

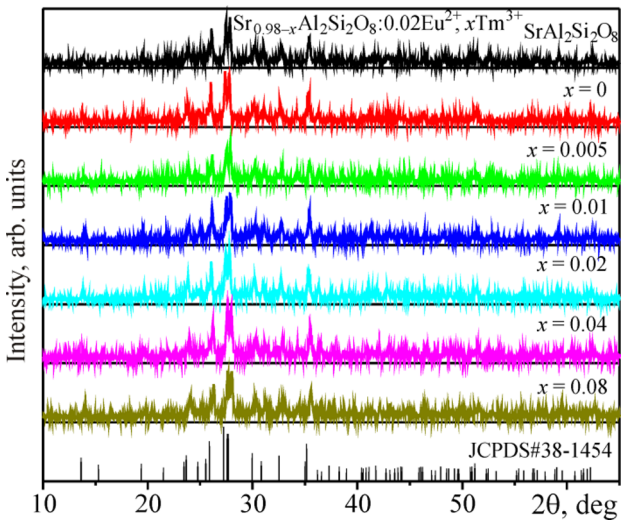

Fig. 1. XRD diffraction pattern of $Sr_1Al_2Si_2O_8$, $Sr_{0.98-x}Al_2Si_2O_8$:0.02Eu^{2+}, xTm^{3+} (x = 0, 0.005, 0.01, 0.02, 0.04, 0.08) samples with a standard JCPDS card (No. 38-1454).

Sample characterization and equipment

The crystal structure and phase compositions of the samples were analyzed in a Shimadzu XRD-6000 powder diffractometer. Cu Kα was used as a radiation source. The step scan speed was 4°/min and the scanning angle – 0.02°/s. The selected scan range was from 10° to 65°. An F-4600 fluorescence spectrometer produced by Hitachi, Ltd. was used to measure the emission and excitation spectra, the afterglow attenuation, and the optical excitation attenuation of the sample. Before performing a photostimulated decay test, the sample was irradiated with a 365 nm ultraviolet light for 5 minutes and left intact for 20 minutes (to eliminate the effect of long afterglow on the test). It was excited by a 980 nm laser at 1 mW. The measurement of pyroluminescence was carried out using a DMU-450 temperature control system independently developed by the Dalian Maritime University. The sample was irradiated for 5 minutes under UV365 and its pyroluminescence was measured 3 minutes after irradiation within the temperature interval of 300–700 K.

RESULTS AND DISCUSSION

X-ray diffraction (XRD) phase analysis

In order to analyze all six experimental samples of $Sr_1Al_2Si_2O_8$, $Sr_{0.98}Al_2Si_2O_8$:0.02Eu^{2+} and $Sr_{0.98-x}Al_2Si_2O_8$:0.02Eu^{2+}, xTm^{3+} (x = 0.005, 0.01, 0.02, 0.04, 0.08) $Sr_{0.98-x}Al_2Si_2O_8$, we performed XRD characterization on a series of samples, providing the information related to crystallinity, lattice orientation, and sample purity. All samples were characterized by an XRD-6000 powder diffractometer. The results are shown in Fig. 1.

Figure 1 presents the XRD diffraction spectra of $Sr_1Al_2Si_2O_8$, $Sr_{0.98}Al_2Si_2O_8$: 0.02Eu^{2+} and $Sr_{0.98-x}Al_2Si_2O_8$: 0.02Eu^{2+}, xTm^{3+} (x = 0.005, 0.01, 0.02, 0.04, 0.08) samples obtained using a standard JCPDS card (No. 38-1454). The $Sr_1Al_2Si_2O_8$ sample synthesized in this experiment belongs to the triclinic system, and the space group is C2/m [28]. It can be concluded from Fig. 1 that the prepared phosphor sample is basically consistent with the standard PDF card diffraction peak intensity, peak position and FWHM, and there are no other peaks. The prepared experimental samples

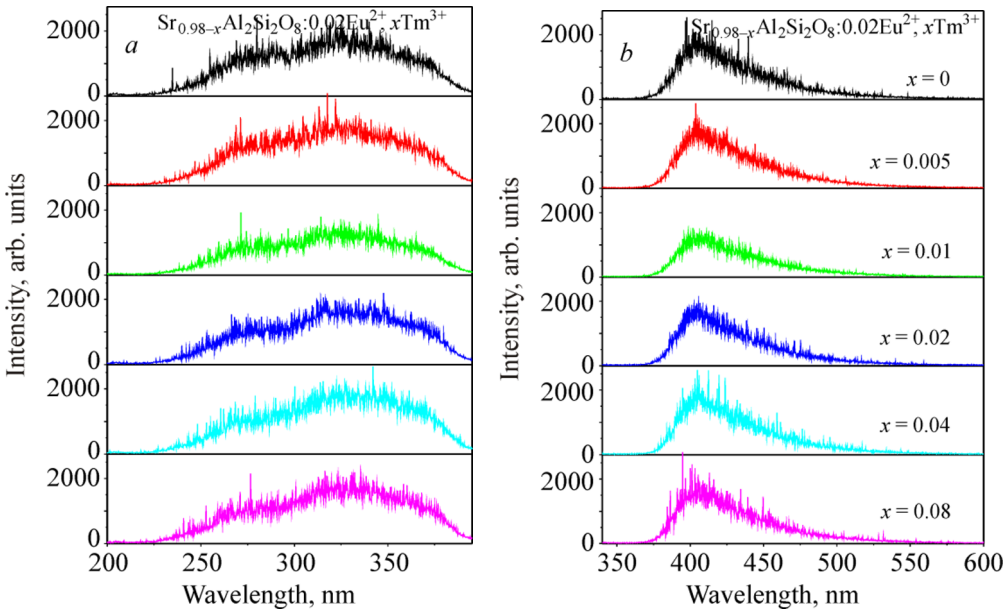

Fig. 2. Excitation and emission spectra of $Sr_{0.98}Al_2Si_2O_8$:0.02Eu^{2+} and (x = 0.005, 0.01, 0.02, 0.04, 0.08) $Sr_{0.98-x}Al_2Si_2O_8$ samples.

showed good lattice orientation and crystallinity, and their doping with Eu^{2+} and Tm^{3+} did not change the crystal structure of $Sr_1Al_2Si_2O_8$. The Eu^{2+} and Tm^{3+} dopants in the resulting sample have completely replaced Sr^{2+}.

Emission and excitation spectrum analysis

In order to obtain more information on the luminescence properties, the sample was tested under a 400 V voltage 5 nm slit using an F-4600 fluorescence spectrometer to obtain its excitation spectrum as shown in Fig. 2*a* below. It can be seen that the main excitation peak of $Sr_1Al_2Si_2O_8$, $Sr_{0.98}Al_2Si_2O_8$:0.02Eu^{2+}, $x$$Tm^{3+}$ (x = 0, 0.005, 0.01, 0.02, 0.04, 0.08) is located at 330 nm. This indicates that the sample can be excited by its broadband in the 280–390 nm ultraviolet region. Moreover, the excitation spectra of Eu^{2+} and Tm^{3+} do not change the position of the main peak of 330 nm, indicating that a divalent Eu ion acts as the luminescent center due to the $^4f_6{}^5d_1$-$^4f_7$ transition [29]. Figure 2*b* shows the emission spectrum of the sample. The luminescence range is mainly in the blue region of 375–475 nm, and the main peak is at 405 nm. After an ultraviolet excitation, a strong blue light can be observed by the naked eye.

According to the above emission spectrum, the sample composition is as follows: $Sr_{0.98-x}Al_2Si_2O_8$:0.02Eu^{2+}, $x$$Tm^{3+}$ (x = 0, 0.005, 0.01, 0.02, 0.04, 0.08). The main peak positions of $Sr_{0.98-x}Al_2Si_2O_8$ are all blue light at 405 nm. This is similar to the sample luminescence center of $Sr_3Al_{10}SiO_{20}$:Eu^{2+} given by Li et al. at 429 nm [30]. Van Uitert [35] studied the relationship between the 5d coordination number and the excited position of the aluminosilicate system [31], which can have the following formula:

$$E = Q\left[1-\left(\frac{V}{4}\right)^{\frac{1}{V}}\cdot 10^{-\frac{n\cdot r\cdot E_A}{80}}\right]. \quad (1)$$

To further simplify the calculation, the formula can be reconstructed by taking the logarithm on both sides to obtain

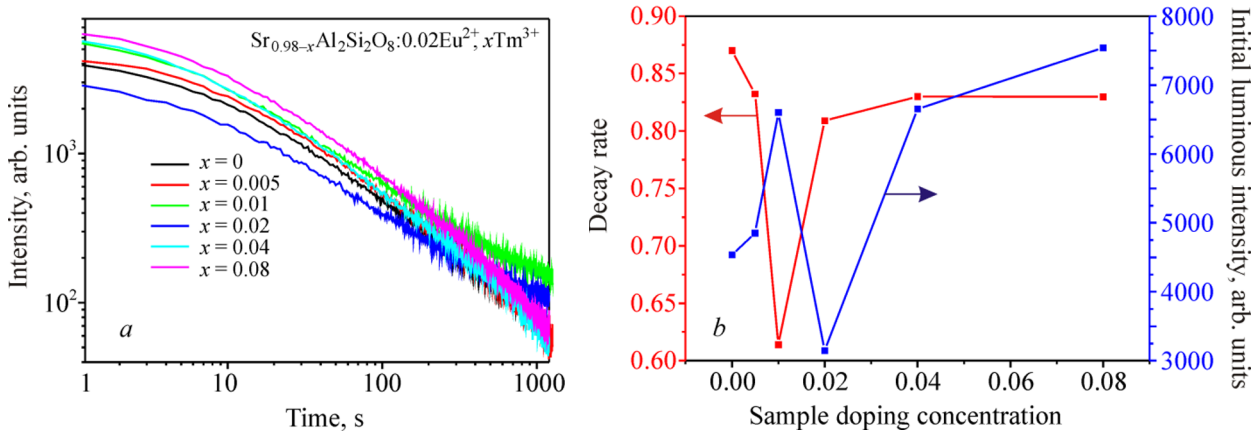

Fig. 3. Afterglow decay curves of different samples (*a*), curves of dependence between initial concentration and decay rate for samples with different dopant concentrations (*b*).

$$n \cdot r = -\frac{80}{E_A} \log\left[\left(1-\frac{E}{Q}\right)\cdot\left(\frac{V}{4}\right)^{-\frac{1}{V}}\right], \tag{2}$$

where n represents the coordination number, r represents the ionic radius (nm), E_A is the electron affinity (eV) with the anion coordination atom, E represents the low energy band position (cm^{-1}) of the 5d excited state, and Q represents the free ion in the energy position of the low d band edge, and V is the activator ion valence. The main peak position of the emission spectrum of $Sr_{0.98}Al_2Si_2O_8$:$0.02Eu^{2+}$ activation material is 405 nm, the corresponding Q is 24691 cm^{-1}, and the valence of Eu ion is 2, so V is 2. According to the literature [29], E_A takes the value of 2.19 eV and comprehensively calculates nr = 15.0526. Considering comprehensively, the coordination number n = 12, $r(Sr^{2+})$ = 0.126 nm. The theoretical value is 15.12, which is closest to the experimental value. An actual value of Eu^{2+} was calculated as the illuminating center position according to the theoretical value to be 404.36 nm.

Long decay afterglow analysis

Figure 3*a* shows the afterglow decay curves from the $Sr_{0.98-x}Al_2Si_2O_8$:$0.02Eu^{2+}$, xTm^{3+} and (x = 0, 0.005, 0.01, 0.02, 0.04, 0.08) samples 5 min after their irradiation with the UV light (based on the spectrometric data). The afterglow attenuation curve was measured at a 1200 s afterglow attenuation. It can be seen from the Fig. 3 that the afterglow decay rate of Tm^{3+} doping somewhat decreases compared with undoped Tm^{3+}. Furthermore, when the Tm^{3+}doping is 1%, the attenuation is the slowest and the decay rate is the lowest. According to the long afterglow decay rate formula proposed by Wang et al. [31],

$$I = A \cdot t^{-\alpha} \tag{3}$$

In formula (3), A represents the fitting constant, t represents the fluorescence decay time, I represents the initial luminescence intensity, and α represents the rate at which the sample decays. Using formula (3), one can obtain the relationship between the initial luminescence intensity and the decay rate of the samples of different concentrations in Fig. 3*b*. We can obtain the decay rate for the $Sr_{0.97}Al_2Si_2O_8$:$0.02Eu^{2+}$ sample after fitting; the decay rate for $0.01Tm^{3+}$ in 1200 s is 0.61389, which is the slowest decay rate among all samples.

In order to further verify the afterglow effect for the experimental samples, the afterglow emission spectrum of the F-4600 fluorescence spectrometer was tested. Figure 4*a* shows the $Sr_{0.98}Al_2Si_2O_8$:$0.02Eu^{2+}$ and $Sr_{0.97}Al_2Si_2O_8$:

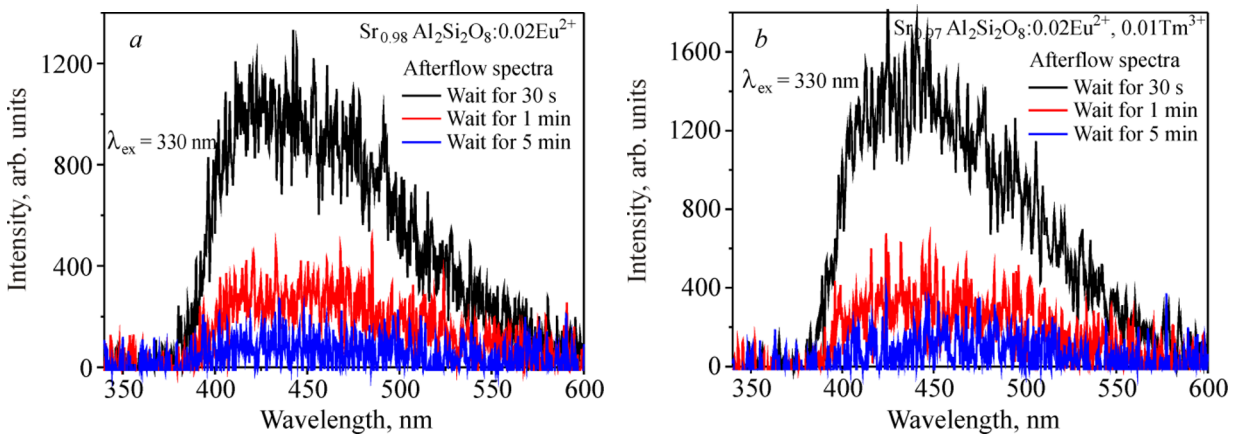

Fig. 4. Afterglow emission spectra from $Sr_{0.98}Al_2Si_2O_8$:0.02Eu^{2+} (*a*) and $Sr_{0.97}Al_2Si_2O_8$:0.02Eu^{2+}, 0.01Tm^{3+} (*b*) samples.

0.02Eu^{2+}, 0.01Tm^{3+} samples emitting a high-intensity blue light at 405 nm, which is the same as the fluorescence emission spectrum. The doping with Tm^{3+} did not change the luminescence center of the afterglow spectrum.

Thermoluminescence spectrum measurement

For many trap distributions and properties, the method of thermoluminescence measurement is considered to be the most ideal one. Pyroluminescence is the phenomenon of luminescence that occurs when an experimental sample is heated. In the study of storage materials, it is important to measure the thermoluminescence peak position, which can characterize the trap level, the radiation recombination and the storage capacity of the sample. Therefore, in order to more clearly understand the trap levels of the experimental $Sr_{0.98}Al_2Si_2O_8$:0.02 Eu^{2+} and (x = 0.005, 0.01, 0.02, 0.04, 0.08) $Sr_{0.98-x}Al_2Si_2O_8$ samples, we tested their thermoluminescence. At a room temperature of 30°C, we irradiated the samples with a 365 nm UV lamp for 5 min, and turned it off 5 min later (excluding the electrons trapped by a shallow trap at room temperature). The heating rates during the measurements were 0.2 K/s, 0.5 K/s, 0.7 K/s, 1.0 K/s, 1.4 K/s, and the measurement temperature range was 300–700K. The curve of the thermoluminescence intensity versus temperature was recorded. The pyroluminescence curve of Fig. 5*a*, *b*, *c*, *d*, *e* was obtained as follows.

The thermoluminescence spectra in Fig. 5*a*, *b*, *c*, *d*, *e*, *f* suggest that the samples are doped with different concentrations of Tm^{3+} compared to the undoped Tm^{3+} sample. The theory states that the higher the temperature of the main T_m peak, the stronger the ability of electrons to trap the carriers and the deeper the trap. Although there is no new trap in the co-doped sample, the temperature T_{max} increases significantly and the pyrolysis peak width becomes wider. The ability of the co-doped sample electrons to trap the carriers becomes stronger and the concentration becomes higher, so that the initial irradiation intensity of the same-intensity photoexcited light source is stronger than that of the single-doped $Sr_{0.98}Al_2Si_2O_8$:0.02Eu^{2+} sample, which is a marked increase. Note that there may be a superior photostimulated performance.

In order to further visualize the change of the trap level of the single-doped and the co-doped samples, the method of variable heating rate is used to calculate the trap depth E, which is expressed by the following formula [32–34]:

$$\ln(T_{max}^2/\beta) = E/kT_m + \ln(E/ks[1 + (b - 1)\Delta]), \quad (4)$$

wherein β represents the heating rate in K/s, T_{max} represents the temperature corresponding to the value of the highest spectral intensity, E represents the trap depth (eV) of the sample, b represents the kinetic level, k is the Boltzmann

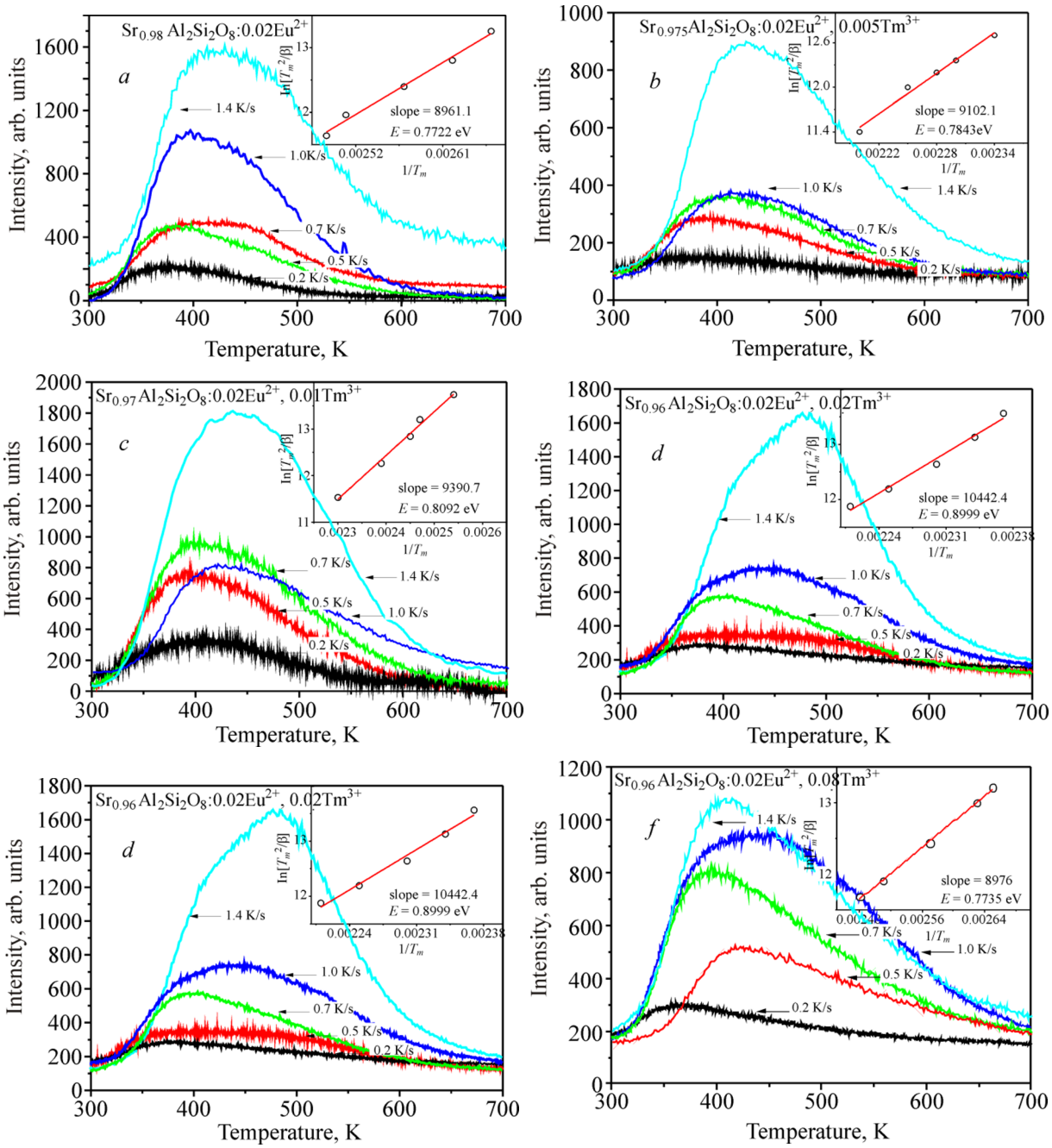

Fig. 5. Thermoluminescence spectra of $Sr_{0.98}Al_2Si_2O_8$:0.02Eu^{2+} and (x = 0.005, 0.01, 0.02, 0.04, 0.08) $Sr_{0.98-x}Al_2Si_2O_8$ samples.

constant, and s represents the frequency factor. According to the calculation and analysis, we can tabulate the data for six samples in Table 1.

It can be seen from Table 1 that the co-doped $Sr_{0.98-x}Al_2Si_2O_8$:0.02Eu^{2+}, $x$$Tm^{3+}$ (x = 0, 0.005, 0.01, 0.02, 0.04, 0.08) sample has a higher trap level than that of the $Sr_{0.96}Al_2Si_2O_8$:0.02Eu^{2+} single-doped sample. Note that the trap level of $Sr_{0.96}Al_2Si_2O_8$:0.02Eu^{2+}, 0.02Tm^{3+} sample is close to 0.9 eV. This also indicates that the weak fluorescence and afterglow are due to the shallow trap pre-release at room temperature.

TABLE 1. Slope, Intercept and Trap Depth Factor Corresponding to Samples *a–f*

Samples	E/k, K	$\ln(E/ks[1 + (b - 1)\Delta])$	E, eV
$Sr_{0.98}Al_2Si_2O_8$:0.02Eu^{2+}	8961.1	–10.6177	0.7722
$Sr_{0.975}Al_2Si_2O_8$:0.02Eu^{2+}, 0.005Tm^{3+}	9102.1	–8.5657	0.7843
$Sr_{0.97}Al_2Si_2O_8$:0.02Eu^{2+}, 0.01Tm^{3+}	9390.7	–10.1042	0.8092
$Sr_{0.96}Al_2Si_2O_8$:0.02Eu^{2+}, 0.02Tm^{3+}	10442.4	–11.2749	0.8999
$Sr_{0.94}Al_2Si_2O_8$:0.02Eu^{2+}, 0.04Tm^{3+}	9021.1	–10.7443	0.7784
$Sr_{0.9}Al_2Si_2O_8$:0.02Eu^{2+}, 0.08Tm^{3+}	8976	–10.6104	0.7735

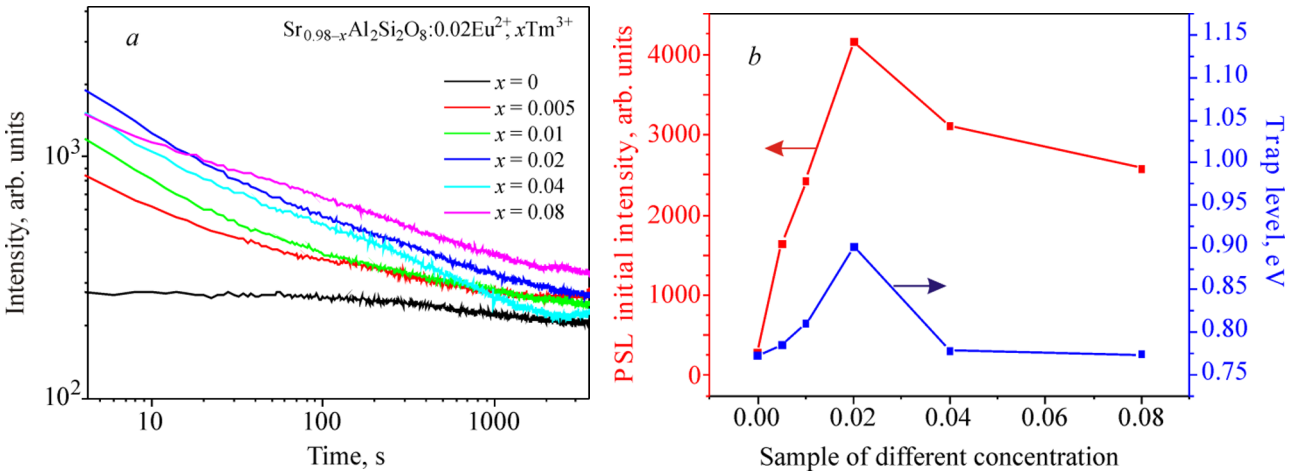

Fig. 6. Photostimulable luminescence attenuation curves from $Sr_{0.98}Al_2Si_2O_8$:0.02Eu^{2+} and (x = 0.005, 0.01, 0.02, 0.04, 0.08) $Sr_{0.98-x}Al_2Si_2O_8$ samples (*a*). Relationship between photoexcitation luminescence and trap energy level for $Sr_{0.98}Al_2Si_2O_8$:0.02Eu^{2+} and (x = 0.005, 0.01, 0.02, 0.04, 0.08) $Sr_{0.98-x}Al_2Si_2O_8$ samples (*b*).

Photostimulable luminescence test

It is important to further study the carriers trapped by the deep trap electrons of the material for it to be effectively used as a photostimulated luminescent material. We irradiated the sample with a 365 nm UV lamp for 5 min and placed it in a darkroom for 20 min to eliminate the effect of long afterglow luminescence on the optical excitation test. The sample was irradiated with a 980 nm infrared laser at a power of 1 mW, and the initial excitation intensity of the photostimulated luminiscence was recorded; the photostimulated attenuation curve is shown in Fig. 6.

The initial intensity of photostimulated illumination is an important indicator of the optical storage performance. It can be seen from Fig. 6*a* that as the concentration of Tm^{3+} as a co-dopant is increased, the initial luminescence intensity first tends to increase and then decreases. The highest value is 4154 for the $Sr_{0.96}Al_2Si_2O_8$:0.02Eu^{2+}, 0.02Tm^{3+} sample. The attenuation process can be divided into two stages: fast and smooth attenuation. The fast attenuation stage is 1000 times faster than the stationary attenuation. No such phenomenon was observed in the single-doped $Sr_{0.98}Al_2Si_2O_8$:0.02Eu^{2+} sample. This has a certain regular relationship with the electron trap generated by the previous thermoluminescence. As can be seen from Fig. 6*b*, as the trap deepens the initial intensity of the photostimulated luminescence increases significantly. The decrease in the case, where the limit value of the initial excitation of the photostimulation is reached, is because the annihilation center formed by the Sr^{2+} vacancy increases the luminescence of the photostimulated and the thermal luminescence T_{max} as the concentration increases.

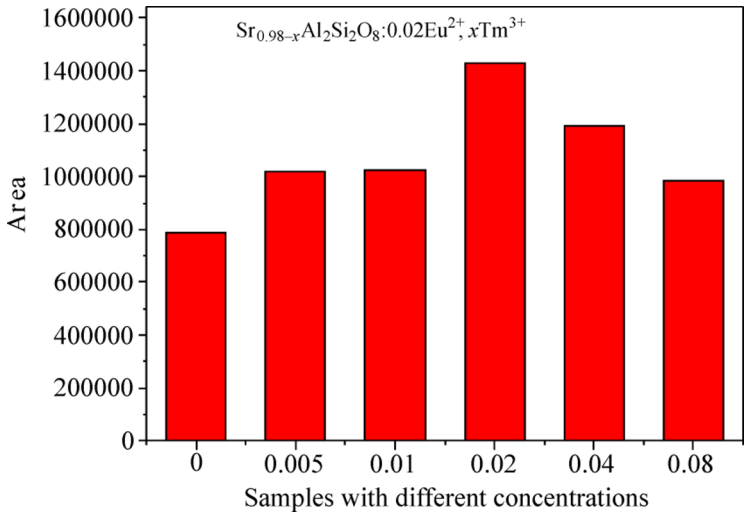

Fig. 7. Comparison of optical and storage reserves of $Sr_{0.98}Al_2Si_2O_8$:$0.02Eu^{2+}$ and (x = 0.005, 0.01, 0.02, 0.04, 0.08) $Sr_{0.98-x}Al_2Si_2O_8$ samples.

Photostimulable luminescence storage calculation

The amount of light stored in the light excitation is the amount of photons emitted by the light excitation. The theory confirms that light increases with the amount of electrons generated in deep traps [34].

$$\int_{t_0}^{t} I(t)dt = -an_t \ . \tag{5}$$

According to equation (5), we can draw a conclusion that the amount of optical excitation storage can be expressed by applying the area of photostimulated attenuation and time integration. The optical storage of the $Sr_{0.98}Al_2Si_2O_8$: $0.02Eu^{2+}$ and $Sr_{0.98-x}Al_2Si_2O_8$: $0.02Eu^{2+}$, xTm^{3+} (x = 0.005, 0.01, 0.02, 0.04, 0.08) samples can be as shown in Fig. 7.

It is evident from Fig. 7 that the amount of light storage first increases and then decreases with the increase of co-doped Tm^{3+}. Compared with the single-doped sample, the co-doped sample has a significant improvement: specifically, the optical storage reserve of the 2% Tm^{3+}-doped sample is 1.8 times that of the Eu^{2+}single-doped one. To sum up, the optical storage performance of the sample has been significantly improved.

Long afterglow luminescence

Based on the experimental analysis and the excellent results obtained, Fig. 8 proposes a model for the long-lasting phosphorescence process in $Sr_1Al_2Si_2O_8$ with Eu^{2+} as the luminescent center. This provides insight into the electron trapping process that occurs in the rare-earth ion-doped matrices acting as luminescent centers and exhibiting long-lasting phosphorescence phenomena.

When the sample is exposed to external UV radiation, electrons are excited to the excited state through transitions. Some of these electrons return to the ground state of Eu^{2+} and recombine with the holes, resulting in characteristic emission peaks of Eu^{2+}. The remaining electrons are trapped and temporarily stored in the trap sites.

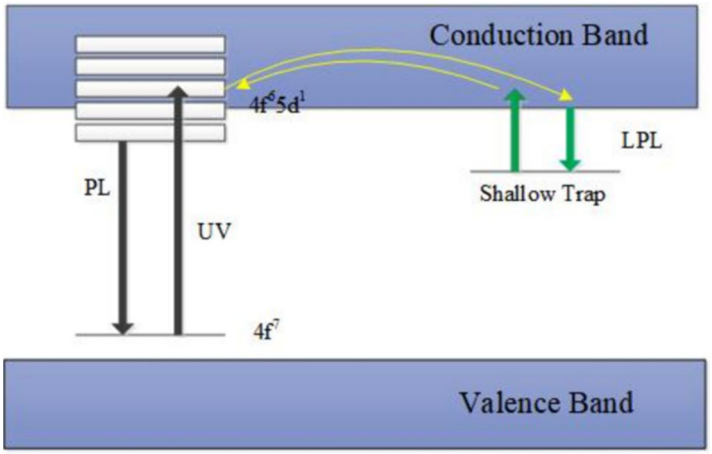

Fig. 8. A simplified model of the long-lasting phosphorescence process.

When subjected to thermal perturbations, these trapped electrons are released from the trap sites and emitted at a certain wavelength in the luminescence center, leading to the phenomenon of long-lasting phosphorescence.

CONCLUSIONS

The samples of $Sr_{0.98-x}Al_2Si_2O_8$:0.02Eu^{2+}, xTm^{3+} (x = 0, 0.005, 0.01, 0.02, 0.04, 0.08) have been successfully prepared by the high-temperature solid-phase method. The fluorescence excitation and emission spectra of the samples, the coordination numbers of Sr^{2+}, the thermoluminescence and photoexcitation performance have been given an in-depth analysis and the following conclusions have been drawn:

(1) According to the XRD test performed in this study, a high-purity phosphor of an excellent crystallinity can be prepared by an exposure to a temperature of 1350°C for 4 hours. The phosphor can be excited by a broadband of 280 nm to 390 nm with a peak wavelength of 330 nm. There is a strong blue light emission at the peak wavelength of 405 nm in the emission spectrum.

(2) In the afterglow attenuation curve obtained by the test, the decay rate of the co-doped Tm^{3+} sample is smaller than that of the single-doped Eu^{2+} sample, specifically the $Sr_{0.97}Al_2Si_2O_8$:0.02Eu^{2+}sample, and the decay rate of 0.01Tm^{3+} is the smallest. It is as low as 0.61389.

(3) The relationship between the 5d coordination number and the excited edge position in the aluminosilicate system was studied according to Van Uitert [35]. The experimental sample of the aluminosilicate system with Eu as the luminescent center was calculated, and the divalent Eu ion replaced Sr^{2+} with the coordination number of 12, and $r(Sr^{+})$ = 0.126 nm.

(4) After doping with different Tm^{3+}concentrations, $Sr_{0.98}Al_2Si_2O_8$:0.02Eu^{2+} exhibits a deeper trap level on the original basis, specifically $Sr_{0.96}Al_2Si_2O_8$:0.02Eu^{2+}, and the deepest thermoluminescence trap level of 0.02Tm^{3+} is 0.99 eV.

(5) In the optical storage performance test, the initial intensity of photoexcitation luminescence of the co-doped sample was significantly improved: compared with the Eu^{2+} single-doped sample, the $Sr_{0.96}Al_2Si_2O_8$:0.02Eu^{2+}, 0.02Tm^{3+} sample had a factor of 1000 higher intensity. The amount of light storage is 1.8 times that of a single doped sample.

Therefore, $Sr_{0.97}Al_2Si_2O_8$:0.02Eu^{2+}, 0.01Tm^{3+} is a promising long afterglow-blue phosphor because of its lowest decay rate. The $Sr_{0.96}Al_2Si_2O_8$:0.02Eu^{2+}, 0.02Tm^{3+} samples are suitable for new white LED blue phosphors excited by broadband in the near ultraviolet, and are also potential optical information storage materials.

ACKONWLEDGEMENT

This work has been funded by the National Natural Science Foundation of China (approval number: 52201065)

REFERENCES

1. Q. Shao, H. Lin, Y. Dong, Y. Fu, C. Liang, and J. He, J. Solid State Chem., **72–77**, 225 (2015).
2. X. Yu, T. Wang, X. Xu, D. Zhou, and J. Qiu, ECS Solid State Lett., **R4–R6**, 3 (2013).
3. F. Liu, W. Yan, Y.J. Chuang, Z. Zhen, J. Xie, and Z. Pan, Sci. Rep., **1554–1563**, 3 (2013).
4. X. Liu, J. Zhang, X. Zhang, Z. Hao, J. Qiao, and X. Dong, Opt. Lett., **148–150**, 38 (2013).
5. X. Xu, Q. He, and L. Yan, J. Alloys Compd., **22–26**, 574 (2013).
6. A. McAulay, J. Wang, and C. Ma, Proc. SPIE, **271–276**, 77 (1989).
7. Z. Wen, N. H. Farhat, and Z. J. Zhao, Appl. Opt., **7251–7265**, 32 (1993).
8. H. Yu, G. Xiong, and J. Ma, J. TIT, **18–23**, 17 (2001).
9. W. Jiang, Z. Xu, and X. Zhang, Sm. Mater. Lett., **1042–1045**, 61 (2007).
10. A. S. Pradhan, J. I. Lee, and J. L. Kim, Med. Phys., **85–99**, 33 (2008).
11. H. B. Liu, B. L. Feng, L. Luo, C. L. Han, and P. A. Tanner, Opt. Mater. Express, **3375–3385**, 6 (2016).
12. Y. X. Zhuang, Y. Lv, L. Wang, W. W. Chen, T. L. Zhou, T. Takeda, N. Hirosaki, and R. J. Xie, ACS Appl. Mater. Interfaces, **1854–1864**, 10 (2018).
13. Y. X. Zhuang, Y. Lv, Y. Li, T. L. Zhou, J. Xu, J. Ueda, S. Tanabe, and R. J. Xie, Inorg. Chem., **11890–11897**, 55 (2016).
14. L. Xiao, J. Zhou, G. Z. Liu, and L. Wang, J. Alloys Compd., **24–29**, 712 (2017).
15. S. Hufner and B. Judd, NY Acad. Press, **87–95**, 32 (1979).
16. J. Wu, N. Wang, V. Yan, and H. Wang, Nano Res., **1863–1877**, 14 (2021).
17. A. Lecointre, A. Bessiere, A. Bos, and P. Dorenbos, J. Phys. Chem. C, **4217–4227**, 115 (2011).
18. P. Dorenbos, J. Lumin., **155–176**, 91 (2000).
19. F. Clabau, A. Garcia, P. Bonville, D. Gonbeau, T. Le Mercier, P. Deniard, and S. Jobic. J. Solid State Chem., **1456–1461**, 181 (2008).
20. M. Ma, D. Zhu, C. Zhao, T. Han, S. Cao, and M. Tu, Opt. Commun., **665–668**, 285 (2012).
21. S. C. Gadam and S. Dhoble, J. Lumin., **23–26**, 14 (2013).
22. Y. Kojima, T. Aoi, and U. Tetsuo, J. Lumin., **42–45**, 146 (2014).
23. O. Y. Manashirov, E. M. Zvereva, V. B. Gutan, A. N. Gorgobiani, S. A. Ambrozevic, and A. N. Lobanov, Inorg. Mater., **487–491**, 49 (2013).
24. S. Shuang, D. Kai, K. Huang, and L. Cheng, Adv. Powder Technol., **1516–1519**, 25 (2014).
25. Z. Hua, L. Salamanca-Riba, M. Wuttig, and P. K. Soltani, J. Opt. Soc. Am. B, **1464–1469**, 10 (1993).
26. M. V. Nadezhkin, D. V. Orlova, S. A. Barannikova, and N. M. Mnikh, Russ. Phys. J., **65**, No. 3, 507 (2022).
27. Z. Zhang, X. Xu, and J. Qiu, Spectrosc. Spectral Anal., **1486–1491**, 34 (2014).
28. X. Sun, J. Zhang, X. Zhang, Y. Luo, and Z. Hao, J. Appl. Phys., **013501**, 105 (2009).
29. F. Wang, Y .G. Tian, and Q. Zhang, J. Optoelectron. Laser, **1520–1525**, 26 (2015).
30. P. Li, Z. Yang, and Z. Wang, Chin. Sci. Bull., **973–977**, 53 (2008).
31. R. Chen, Phys. J. Electrochem. Soc., **1254–1257**, 116 (1969).
32. M. Wang, X. Zhang, and Z. Hao, Opt. Mater., **1042–1045**, 32 (2010).
33. A. H. Krumpel and E. V. Kolk, J. Appl. Phys., **073505–073514**, 104 (2008).
34. X. Liu, J. Zhang, X. Zhang, Z. Hao, J. Qiao, and X. Dong, Opt. Lett., **148–150**, 38 (2013).
35. L. G. Van Uitert, J. Lumin., **1–9**, 29 (1984).